Published in final edited form as:
Eur Biophys J. 2015 February ; 44(0): 91–102. doi:10.1007/s00249-014-1004-7.

Properties of membranes derived from the total lipids extracted from clear and cataractous lenses of 61–70-year-old human donors

Laxman Mainali,
Department of Biophysics, Medical College of Wisconsin, 8701 Watertown Plank Road, Milwaukee, WI 53226, USA

Marija Raguz,
Department of Biophysics, Medical College of Wisconsin, 8701 Watertown Plank Road, Milwaukee, WI 53226, USA

Department of Medical Physics and Biophysics, School of Medicine, University of Split, Split, Croatia

William J. O'Brien, and
Department of Ophthalmology, Medical College of Wisconsin, Milwaukee, WI 53226, USA

Witold K. Subczynski
Department of Biophysics, Medical College of Wisconsin, 8701 Watertown Plank Road, Milwaukee, WI 53226, USA

Abstract

Human lens-lipid membranes prepared from the total lipids extracted from clear and cataractous lens cortexes and nuclei of 61–70-year-old donors by use of a rapid solvent-exchange method were investigated. The measured cholesterol-to-phospholipid (Chol/PL) molar ratio in these membranes was 1.8 and 4.4 for cortex and nucleus of clear lenses, respectively, and 1.14 and 1.45 for cataractous lenses. Properties and organization of the lipid bilayer were investigated by use of electron paramagnetic resonance spin-labeling methods. Formation of Chol crystals was confirmed by use of differential scanning calorimetry. Pure cholesterol bilayer domains (CBDs) were formed in all the membranes investigated. It was shown that in clear lens membranes of the nucleus, Chol exists in three different environments: (1) dispersed in phospholipid bilayers (PCDs), (2) in CBDs, and (3) in Chol crystals. In clear lens membranes of the cortex, and in cortical and nuclear cataractous lens membranes, Chol crystals were not detected, because of the lower Chol content. Profiles of membrane properties (alkyl-chain order, fluidity, oxygen transport, and hydrophobicity) across the PCD were very similar for clear and cataractous membranes. Profiles of the oxygen transport parameter across the CBD were, however, different for cortical clear and cataractous membranes—the amount and size of CBDs was less in cataractous membranes. These results suggest that high Chol content, formation of CBDs, and formation of

subczyn@mcw.edu.

Chol crystals should not be regarded as major predispositions for the development of age-related cataracts.

Keywords

Cholesterol; Cholesterol crystals; Membrane domains; Hydrophobic barrier; Oxygen permeation; Spin labeling

Introduction

The membranes of the fiber cells from which the human eye lens is built are overloaded with cholesterol, which not only saturates the phospholipid bilayer but also leads to formation of cholesterol bilayer domains (CBDs) within these membranes (Jacob et al. 1999; Mainali et al. 2013b). These domains have also been called cholesterol crystalline domains (Jacob et al. 1999, 2001). Among the elderly, the cholesterol content of lens membranes is often high enough to induce formation not only of CBDs but also cholesterol crystals, presumably outside the fiber cell membranes (Mason et al. 2003). It is not clear if the high Chol content and the appearance of CBDs and/or Chol crystals are harmful or beneficial to lens function, especially lens transparency (Borchman et al. 1996; Jacob et al. 1999; Mason et al. 2003; Tulenko et al. 1998). The significance of cholesterol in the eye lens is emphasized by observations that inherited defects in cholesterol metabolism enzymes and use of cholesterol-biosynthesis-inhibiting drugs cause cataract formation in animals and humans (Borchman et al. 1989; Cenedella 1996; de Vries and Cohen 1993; Kirby 1967; Mosley et al. 1989). These earlier observations were recently confirmed by retrospective cohort studies comparing the risk of development of cataracts between statin users and non-users which showed that the risk of cataract development was increased among statin users (Lai et al. 2013; Leuschen et al. 2013; Machan et al. 2012).

Our research is focused on developing a better understanding cholesterol functions at a molecular level. We are concerned with cholesterol-induced changes in the properties and organization of the lipid bilayer of the fiber cell plasma membrane. We have investigated membranes with lipid compositions resembling those of the eye lenses of different species (Mainali et al. 2012a, 2013b; Raguz et al. 2009) and lens-lipid membranes formed from lipids extracted from the eyes of different species, donors of different age, and different regions of the eye lens (Mainali et al. 2012a, 2013b; Raguz et al. 2008, 2009; Widomska et al. 2007). Previous research, summarized in a review by Subczynski et al. (2012), has enabled identification of a substantial number of cholesterol functions specific to the fiber cell plasma membrane. The CBD is of crucial importance. The presence of CBDs provides buffering capacity for the cholesterol concentration in the surrounding phospholipid bilayer, keeping it at a constant saturating level. The saturating cholesterol content of fiber cell membranes keeps the bulk physical properties of lens-lipid membranes consistent and independent of changes in phospholipid composition. Thus, the CBD helps to maintain lens membrane homeostasis when the membrane phospholipid composition changes significantly during aging (Borchman et al. 1994; Deeley et al. 2008; Yappert and Borchman 2004;

Yappert et al. 2003) and as a result of disease (Borchman et al. 1993; Huang et al. 2005; Paterson et al. 1997).

When the Chol content exceeds the Chol solubility threshold, Chol crystals are formed, presumably outside the membrane (Epand 2003; Huang et al. 1999). We were able to show, by using the rapid solvent exchange method for liposome preparation (Buboltz 2009), that formation of CBDs precedes formation of Chol crystals (Mainali et al. 2013c). We believe this very significant discovery enables better understanding of the positive functions of high membrane cholesterol levels in lens fiber cell membranes (Subczynski et al. 2012) and their negative functions during development of atherosclerosis (Mason and Jacob 2003).

In the studies reported here we extended our investigations of the properties of lens-lipid membranes made of lipids isolated from the clear lenses of 41–60-year-old human donors (Mainali et al. 2013b) to a group of older donors ranging in age from 61 to 70 years. The latter group was sub-divided into donors with either clear or cataractous lenses. This enabled us to seek regional (cortex versus nucleus) and age-dependent changes, and to determine major differences in the organization of lipids in the lens membranes of people with cataracts and in age-matched clear lenses. To obtain a complete set of data about the structure and organization of lipids in lens-lipid membranes, we combined lipids from thirty clear lenses and separately from twelve cataractous lenses. As a result of the development of new electron paramagnetic resonance (EPR) techniques (Mainali et al. 2014) it is possible to obtain the same set of data from samples prepared from the eyes of a single donor. This innovative approach will enable consideration of the donor health history as a major factor in analysis of data.

Please note that these results are based on measurements for lens-lipid membranes prepared from lipids extracted from human lenses, i.e. membranes without a protein component. Intact eye lens membranes are loaded with membrane proteins, and both intrinsic and extrinsic proteins affect the distribution (Rujoi et al. 2003) and properties (Raguz et al. 2014) of the lipid bilayer portion of these membranes. These studies are however an essential step in investigation of the properties and organization of the lipid-bilayer portion of fiber cell plasma membranes. Without this research, it would probably be impossible to understand clearly the mechanisms by which intrinsic and extrinsic proteins affect the properties of the lipid bilayer, as discussed in more detail by Subczynski et al. (2012).

Materials and methods

Materials

1-Palmitoyl-2-(*n*-doxylstearoyl) phosphatidylcholine (*n*-PC, *n* = 5, 7, 10, 12, 14, or 16) and tempocholine-1-palmitoyl-2-oleoylphosphatidic acid ester (T-PC) spin labels were obtained from Avanti Polar Lipids (Alabaster, AL, USA). Cholesterol analogues (androstane spin label, ASL, and cholestane spin label, CSL) and 9-doxylstearic acid spin labels (9-SASL) were purchased from Molecular Probes (Eugene, OR, USA). The structures of the spin labels are reported elsewhere [Fig. 1 in Mainali et al. (2012a) for spin label structures]. Other chemicals of at least reagent grade were purchased from Sigma– Aldrich (St Louis, MO, USA).

Isolation of total lipids from the cortical and nuclear fiber cell membranes of human eye lenses and analysis of lipid composition

Thirty clear and twelve cataractous human lenses were obtained from the Lions Eye Bank of Wisconsin. Eight lenses containing nuclear cataracts, three containing cortical cataracts, and one containing a mixed cortical and nuclear cataract were used. Lens donors ranged in age from 61 to 70 years. Lenses were removed in situ from refrigerated bodies nine hours postmortem, on average. All of the lenses were stored at −80 °C until lipid isolation was performed. Lenses were examined by use of a binocular microscope and were evaluated for color and opacity to determine the presence or absence of cataractous changes. Lenses were accumulated over 4 months, lipid isolation, was were then performed. The cortical and nuclear regions of the lenses were separated on the basis of different tissue consistency (Estrada and Yappert 2004; Rujoi et al. 2003). The total lipids from cortical or nuclear samples were extracted separately by use of minor modifications of the Folch procedure (Folch et al. 1957). Details of these procedures have been described elsewhere (Mainali et al. 2011b). The resulting lipid samples, which were soft, white solids, were stored at −20 °C. Samples were sent to Avanti Polar Lipids (Alabaster, AL, USA) for high-performance liquid chromatography analysis of the total lipid extract. Results for the cortex and nucleus samples of clear lenses, respectively, were: 1.8 and 4.4 for Chol/phospholipid, 0.14 and 0.1 for phosphatidylcholine/phospholipid, 0.66 and 0.78 for sphingomyelin/phospholipid, 0.07 and 0.05 for phosphatidylserine/phospholipid, and 0.12 and 0.06 for phosphatidylethanolamine/phospholipid. Results for the cortex and nucleus samples of cataractous lenses, respectively, were: 1.14 and 1.45 for Chol/phospholipid, 0.11 and 0.17 for phosphatidylcholine/phospholipid, 0.89 and 0.66 for sphingomyelin/phospholipid, and 0.00 and 0.17 for phosphatidylethanolamine/phospholipid. Phosphatidylserine was not detected. The relative abundance of the phospholipid classes in clear lenses were similar to those reported by Deeley et al. (2008) for 60-year-old donors. The Chol/ phospholipid values for clear and cataractous lenses were similar to those reported by Jacob et al. (2001) for 73–80-year-old donors (clear lenses) and for 78–80-year-old donors (cataractous lenses). All these measurements were, however, performed for total lipid extracts without separation for cortical and nuclear samples. Li et al. (1985) evaluated the Chol/phospholipid ratio for consecutive concentric sections of human clear (54–77 year-old donors) and cataractous (65-year-old donor) lenses; for both types of sample the Chol/phospholipid ratio was greater for the nucleus than for the cortex.

Preparation of samples for EPR and differential scanning calorimetry (DSC)

The membranes (multilamellar liposomes) were prepared by use of the rapid solvent exchange method (Buboltz 2009; Buboltz and Feigenson 1999; Huang et al. 1999) with apparatus recently built in our laboratory, and described in detail elsewhere (Buboltz 2009). A chloroform solution of lens lipids with a final volume of 75 μL was added at room temperature to 1.2 mL buffer (10 mM PIPES and 150 mM NaCl, pH 7.0) in a test tube. As described elsewhere (Buboltz 2009), the tube was mounted on a laboratory vortex mixer and coupled to the sample manifold of the rapid solvent exchange device. The vortex mixer was actuated, the flushing-argon flow rate was confirmed, and the manifold valve was quickly opened to a trap-protected vacuum system preset at ~25 torr. After 4 min the vortex mixer

was stopped, the manifold was vented, and the sample tube was removed from the device. The membrane suspensions were then used for EPR and DSC experiments.

EPR measurements

For EPR measurements, membrane suspensions containing 1–2 mg/mL total lipids, to which ~1 mol % spin label (*n*-PC, T-PC, 9-SASL, ASL, or CSL) had been added, were centrifuged briefly (16,000*g*, 15 min, 4 °C), and the loose pellet (~20 % lipid, *w*/*w*) was transferred to a 0.6 mm i.d. capillary made of gas-permeable methylpentene polymer (TPX) and used for EPR measurements (Subczynski et al. 2005). Each membrane sample was prepared from stock solutions, and EPR measurements were completed on the same day. To increase the signal-to-noise ratio, samples were centrifuged in TPX capillaries as described by Subczynski et al. (2005). Conventional EPR spectra were recorded with a Bruker EMX spectrometer equipped with temperature-control accessories. All spectra were obtained at 37 °C. Samples were thoroughly deoxygenated, yielding correct EPR line shapes. The order parameter was calculated on the basis of spectral data measured directly from the spectra, as described elsewhere (Mainali et al. 2011a). Hydrophobicity was determined from spectra of samples frozen at −165 °C, as described by Subczynski et al. (1994).

Spin–lattice relaxation times, T_1 values, of spin labels were determined at 37 °C by analyzing the saturation-recovery signal of the central line obtained by short-pulse saturation-recovery EPR, by use of a laboratory built X-band spectrometer (Kawasaki et al. 2001; Subczynski et al. 1989; Yin and Subczynski 1996). T_1 values for membrane fluidity profiles were determined for thoroughly deoxygenated samples (Mainali et al. 2011a). For measurement of the oxygen transport parameter (Kusumi et al. 1982), samples were equilibrated with the same gas as used for temperature control, i.e., a controlled mixture of nitrogen and air (Kusumi et al. 1982; Subczynski et al. 1992, 2005). In this method, the measured value is the rate of bimolecular collisions between oxygen and the nitroxide group of spin labels expressed as the oxygen transport parameter. This method is extremely sensitive to changes in the local oxygen diffusion–concentration product around the nitroxide group. For measurements of the NiEDDA accessibility parameter, 20 mM NiEDDA was present in the buffer, and saturation-recovery measurements were performed for deoxygenated samples (Raguz et. al 2011a, b). The measured value is the rate of bimolecular collisions between the water-soluble relaxation agent NiEDDA and the nitroxide group of the spin labels. Saturation-recovery signals were fitted by single or double-exponential functions, and data were assigned to an appropriate membrane environment.

DSC measurements

For DSC measurements, samples containing 1 mg/mL of total cortical or nuclear lipids and were used without further centrifugation. Measurements were obtained by use of a Nano DSC with platinum capillary cells obtained from TA instruments. The capillary cell volume was 0.3 mL. The Nano DSCRun operating system software was used to acquire data, and NanoAnalyze software was used for data analysis. A constant scan rate of 1 °/min was used.

Results

Here we present data and discuss the properties of lens-lipid membranes from clear lenses compared with those from cataractous changes. The information is a continuation of previous work on clear lens-lipid membranes from 41–60-year-old human donors. Detailed information regarding processing of the data to obtain profiles of membrane properties can be found elsewhere (Mainali et al. 2013b).

Order and fluidity of phospholipid alkyl chains

It should be noted that the order parameter, which is most often used as a measure of membrane fluidity (Devaux 1983; Schreier et al. 1978), describes the amplitude of the wobbling motion of alkyl-chains relative to the membrane normal and does not explicitly contain time or velocity (Marsh 1981). Thus, this value can be considered non-dynamic. The spin–lattice relaxation rate (T^{-1}_1) obtained from saturation-recovery EPR measurements of lipid spin labels in deoxygenated samples depends primarily on the rotational correlation time of the nitroxide group within the lipid bilayer (Mailer et al. 2005; Robinson et al. 1994). Thus, T^{-1}_1 can be used as a convenient quantitative measure of membrane fluidity that reflects local membrane dynamics (Mainali et al. 2011a, 2013a). Here we use both EPR spectral parameters to describe depth-dependent alkyl-chain organization and dynamics.

Profiles of the order parameter across the phospholipid–cholesterol domain (PCD; the phospholipid cholesterol membrane saturated with Chol before formation of the CBD, or the phospholipid–cholesterol domain coexisting with the CBD) of cortical and nuclear lens-lipid membranes obtained from clear lenses are presented in Fig. 1a; those from cataractous lenses are presented in Fig. 1b. The profiles are practically identical, not only for the cortex and nucleus of clear lenses but also those of cataractous lenses. The fluidity profiles (T^{-1}_1 as a function of depth in the membrane) presented in Fig. 2a, b are also very similar for the cortex and nucleus of clear and cataractous lenses. All these similarities are independent of differences between the phospholipid composition of the membranes indicated in the section “Isolation of total lipids from the cortical and nuclear fiber cell membranes of human eye lenses and analysis of lipid composition”. All the order parameter profiles describing the amplitude of the wobbling motion of the alkyl-chain fragment to which the nitroxide group is attached have an inverted bell-shape and show that alkyl-chain order gradually decreases with depth in the membrane (Fig. 1). As expected, membrane fluidity, described by the dynamics of phospholipid alkyl-chain fragments in Fig. 2, increases toward the center of all the membranes investigated. The similarities of these profiles confirmed our previous finding that the extremely high (saturating) Chol content of the PCD of these membranes determines the order and fluidity of phospholipid alkyl chains, irrespective of different phospholipid composition (Subczynski et al. 2012). The presence of CBDs in all of these membranes (discussed in the section “Discrimination of CBDs using saturation-recovery EPR with Chol analog spin labels”) confirms that their phospholipid bilayer portions are saturated with Chol.

Order and fluidity profiles for membranes with a saturating amount of cholesterol, including those presented in Figs. 1 and 2, differ from profiles across membranes without cholesterol. Values of the order parameter measured at the same depth are always significantly greater

for membranes saturated with cholesterol than for membranes without cholesterol (Fig. 5 in Subczynski et al. 2012). Thus, an ordering effect of cholesterol in lens lipid membranes was observed at all depths from the membrane surface to the membrane center. Fluidity profiles obtained for membranes saturated with cholesterol, compared with fluidity profiles for membranes without cholesterol (Fig. 5 in Subczynski et al. 2012), reveal that cholesterol reduces membrane dynamics only to the depth occupied by the rigid steroid-ring structure and does not change or even increase membrane dynamics at deeper locations. These effects cannot be differentiated by profiles of the order parameter.

Membrane fluidity reported in terms of translational diffusion of molecular oxygen

Profiles of the oxygen transport parameter across the bulk PCD domain of cortical and nuclear lens-lipid membranes from clear (Fig. 3a) and cataractous (Fig. 3b) lenses have a characteristic rectangular shape with an abrupt increase of the oxygen transport parameter between the C9 and C10 positions of the fatty acids of the phospholipids. For all these membranes the oxygen transport parameter from the membrane surface to the depth of C9 is as low as in gel-phase PC membranes; at locations deeper than the C9 it is as high as in fluid-phase membranes (Subczynski et al. 1989, 1991). These profiles are typical for liquid-ordered-phase membranes saturated with Chol and are very different from the bell-shaped profile across model membranes without Chol (Mainali et al. 2012b; Raguz et al. 2008, 2009; Subczynski et al. 2010; Widomska et al. 2007). Similar to profiles of the order parameter (Fig. 1) and the spin–lattice relaxation rate (Fig. 2), profiles of the oxygen transport parameter are almost identical for all these membranes, revealing that the saturating amount of Chol also determines this membrane property.

In profiles of the oxygen transport parameter, membrane organization and fluidity are characterized on the basis of diffusion of molecular oxygen within the membrane, but not directly on the motion and organization of alkyl chains. Profiles of membrane fluidity obtained by these methods differ substantially from typical profiles of membrane fluidity obtained on the basis of alkyl-chain order and dynamics (discussed in the section “Order and fluidity of phospholipid alkyl-chains”), because they reveal more features and have much greater spatial sensitivity. The profiles presented in Fig. 3 indicate that the sharp (~2.5 times) increase in the oxygen transport parameter occurred within the distance of one carbon–carbon bond (i.e., between the C9 and C10 positions along the alkyl-chain). This transition was smooth and profiles of the oxygen transport parameter were bell-shaped for membranes without cholesterol (Fig. 6 in Subczynski et al. 2012). This abrupt change is difficult to explain unless it is assumed that at a saturating cholesterol content:

1. vertical fluctuations of membrane components were much smaller than in membranes without cholesterol;
2. alignment of all membrane components was high; and
3. all cholesterol rings were immersed to the same membrane depth, which was close to the position of C9 in phospholipid alkyl-chains.

Models created by use of molecular dynamics simulations (Plesnar et al. 2012) confirm that saturation with cholesterol narrows the distribution of the vertical positions of atoms in

phospholipid and cholesterol molecules at any bilayer depth and smooths the membrane surface as a result.

Discrimination of CBDs by use of saturation-recovery EPR with Chol analog spin labels

The CBD is a pure Chol domain formed within the PCD (the phospholipid bilayer saturated with Chol) and, for this reason, can be discriminated only with Chol analog spin labels ASL and CSL (Raguz et al. 2011a, b). When located in these two membrane domains, these spin labels alone cannot differentiate between domains, giving similar conventional EPR spectra and similar T_1 values (Raguz et al. 2011a, b). However, the oxygen transport parameter measured with ASL in the center of the CBD is a few times smaller than that measured in the center of the surrounding phospholipid bilayer. Similarly, the NiEDDA accessibility parameter measured with CSL located at the membrane– water interface was a few times greater in the CBD than in the surrounding phospholipid bilayer. These differences were easily detected by using the saturation-recovery EPR approach to confirm the presence of CBDs (Raguz et al. 2011a, b).

Here we have used both approaches to confirm the presence of CBDs in cortical and nuclear lens-lipid membranes from clear and cataractous lenses. These results are illustrated in Fig. 4, which shows representative saturation-recovery signals of ASL in the presence and absence of oxygen in cortical and nuclear lens-lipid membranes obtained from clear and cataractous lenses. For all saturation-recovery signals obtained in the presence of oxygen, only the double-exponential fits were satisfactory, indicating that ASL was located in two environments with different oxygen transport parameters. Results with larger oxygen transport parameters were assigned to the bulk PCD whereas those with smaller oxygen transport parameters were assigned to the CBD. Assignment of saturation-recovery data is discussed in detail by Raguz et al. (2008, 2009, 2011a). Likewise, saturation-recovery signals of CSL in the presence of NiEDDA were also satisfactorily fitted to double exponentials only (data not shown), confirming the existence of CBD within the PCD. Both spin labels were distributed between PCD and CBD, but these domains can be discriminated only with ASL and oxygen as relaxation agent or with CSL and NiEDDA as relaxation agent. Without relaxation agents, saturation-recovery signals of ASL and CSL in membranes were fitted to single exponentials (Fig. 4). Saturation-recovery signals of CSL in the presence of oxygen and those of ASL in the presence of NiEDDA were also satisfactorily fitted with single-exponential curves (data not shown). This indicates that values of the oxygen transport parameter detected with CSL in the PCD and the CBD are very close. The NiEDDA accessibility parameters detected with ASL are close to zero, confirming that NiEDDA does not penetrate to the membrane center where the nitroxide group of ASL is located.

Values of the oxygen transport and NiEDDA accessibility parameters in the discriminated domains are collected in Table 1. We also included values of the oxygen transport parameter obtained with ASL and CSL in the profiles presented in Fig. 3. One of the values of the two oxygen transport parameter obtained with ASL fits the profile across the PCD, confirming correct assignment of the saturation-recovery data. The other value, with that obtained with CSL, enabled us to draw approximate profiles of the oxygen transport parameter across the

CBD for all the membranes investigated (Fig. 3). The results presented in Table 1 and Fig. 3 indicate that the oxygen transport parameter (measured with ASL) and NiEDDA accessibility parameter (measured with CSL) in the CBD in membranes of cataractous lenses differ substantially from those measured in membranes of clear lenses. The oxygen transport parameter in cortical membranes of cataractous lenses is more than twice that in cortical membranes of clear lenses. Similarly, the NiEDDA accessibility parameter in cortical membranes of cataractous lenses is 23 % smaller than that in cortical membranes of clear lenses. These differences in nuclear membranes are not as pronounced as in cortical membranes. The oxygen transport parameter and NiEDDA accessibility parameter sensed, respectively, by the ASL and CSL in the CBD, are properties which can be assigned to the CBD. We showed that for model membranes these properties change substantially with Chol content, because they are close to properties in the surrounding PCD at low Chol content when CBDs start to form (Main-ali et al. 2013c; Raguz et al. 2011a). This suggests that with increased Chol content not only do changes in the relative amounts of CBDs and PCD occur but also the size of the individual CBD domain increases, which reduces the effect of the surrounding PCD. Thus, on the basis of the data presented in Table 1, we can conclude that CBDs in membranes of cataractous lenses are smaller than those in membranes of clear lenses. This difference is more pronounced for cortical membranes. This conclusion correlates with the low Chol content of these membranes, which is significantly lower in cataractous lenses than in clear lenses (as discussed in the section “Isolation of total lipids from the cortical and nuclear fiber cell membranes of human eye lenses and analysis of lipid composition”).

Hydrophobicity of membrane interior

Figure 5a, b show rectangular hydrophobicity profiles across the bulk PCD of cortical and nuclear lens-lipid membranes made of lipids extracted from clear and cataractous lenses. The rectangular shapes, with an abrupt increase of hydrophobicity between C9 and C10, are characteristic of phospholipid membranes saturated with cholesterol (Subczynski et al. 1994). The $2A_Z$ values in the center of all membranes (positions from 10 to 16-PC) indicate that hydrophobicity in this region can be compared with that of hexane and dipropylamine (ε = 2.0–2.9), and hydrophobicity near the membrane surface (position of 5-PC) can be compared with that of methanol and ethanol (ε = 24.3–32.6), although this is still substantially less polar than the bulk aqueous phase (ε = 80). The abrupt increase of hydrophobicity between the C9 and C10 positions was observed for all lens-lipid membranes made from lipids isolated from eye lenses of different species (Main-ali et al. 2012a, 2013b; Raguz et al. 2008, 2009; Widomska et al. 2007). All these membranes have similar high hydro-phobicity in the membrane center (ε = 2.0–2.9). However, the hydrophobicity close to the membrane surface (position of 5-PC) differs from species to species (Mainali et al. 2012a, 2013b; Raguz et al. 2009). The results presented in Fig. 5 show that membranes from cataractous lenses are more polar at the 5-PC position than membranes from clear lenses.

High Chol content is responsible for the rectangular shape of hydrophobicity profiles and for the formation of the highly hydrophobic barrier in lens-lipid membranes. The

hydrophobicity profiles across membranes without cholesterol have a bell-shape with significantly lower hydrophobicity in the membrane centers (Subczynski et al. 1994).

Detection of cholesterol crystals

Figure 6 illustrates the first DSC heating scans for suspensions of lens-lipid membranes used in this investigation. The broad peak at ~86 °C was observed only for the suspension of nuclear lens-lipid membranes from clear lenses. This peak is indicative of conversion of monohydrate Chol crystals to anhydrous Chol crystals (Loomis et al. 1979). The lack of a peak at 36 °C was observed in all scans. A peak at 36 °C would indicate conversion of one crystalline form of anhydrous Chol to another (Benatti et al. 2008; Loomis et al. 1979). This observation is in agreement with data of Huang et al. (1999) and with our own experience (Mainali et al. 2013c) that in membrane suspensions prepared by use of the rapid solvent exchange method only monohydrate Chol crystals are formed. The first heating scans for cortical and nuclear lens-lipid samples from cataractous lenses and for the cortical samples from clear lenses did not show any transitions over a wide temperature range (from 10 to 100 °C), indicating that Chol crystals were not detected.

The cholesterol solubility threshold (CST) determines the Chol content of the lipid bilayer above which Chol crystals start to form. The CST (expressed here as the Chol/ PL molar ratio) differs substantially for major lens phospholipids: for PS membranes the ratio is 1/2 (Bach and Wachtel 2003); for PE membranes it is 1/1 (Shaikh et al. 2006); for PC membranes it is (Huang et al. 1999) 2/1; and for SM membranes it is 2/1 (Epand 2003). Assuming that the CST value in the phospholipid mixture is a weighted sum of individual thresholds with a weight equal to the mole fraction of the individual phospholipid in the mixture (as discussed in the section “Isolation of total lipids from the cortical and nuclear fiber cell membranes of human eye lenses and analysis of lipid composition”), we obtain values of 1.76 and 1.84 for the CST in cortical and nuclear clear lens-lipid membranes and values of 2.00 and 1.83 for the CST in cortical and nuclear cataractous lens-lipid membranes. These values are confirmed by the DSC results presented in Fig. 6. Chol crystals were detected in nuclear clear membranes at a Chol/PL molar ratio of 4.4, which is substantially greater than the evaluated CST value. Chol crystals were not detected for cortical clear membranes or for cortical and nuclear cataractous membranes with Chol/ PL molar ratios of 1.8, 1.14, and 1.45, which are less than or equal to the appropriate values of the CSTs.

Chol crystals can be detected by use of DSC only after a certain amount of Chol has accumulated in these structures. Our evaluations indicate that, in the absence of lipids, the minimum amount of Chol that can be detected in the form of Chol monohydrate crystals when samples are prepared by use of the rapid solvent exchange method is ~0.1 mg/mL. In the presence of phospholipids (DMPC), the sensitivity is ~0.15 mg/mL. To the best of our knowledge, with the exception of our own recent effort (Mainali et al. 2013c), DSC has never previously been used to show the formation of Chol crystals in phospholipid liposome suspensions obtained by use of the rapid solvent exchange method. Instead, Chol crystals were detected using X-ray diffraction for these preparations (Huang et al. 1999). All these measurements indicate that for studies of the organization of membranes saturated and

oversaturated with Chol, liposomes should be prepared by use of the rapid solvent exchange method.

Discussion

We recently published results on the properties of cortical and nuclear human lens-lipid membranes derived from clear lenses of 41–60-year-old donors (Mainali et al. 2013b). Because this age group contains already matured lens fiber cells, and appeared to have not developed detectable cataracts, we use the results of the previous study as a baseline for research on aged lenses. The results presented in this manuscript characterize lenses of 61–70-year-old donors. The major difference from the previous age group was the presence of Chol crystals in the nuclear membranes of clear lenses. Cortical and nuclear membranes of clear lenses for both groups contained CBDs. To the best of our knowledge, this is the first time three different Chol structures (Chol dispersed in the phospholipid bilayer, Chol in CBDs, and Chol in Chol crystals) have been shown to coexist in lens-lipid membranes. Chol crystals were formed only in preparations from aged fiber cells from the nucleus of clear lenses of 61–70-year-old donors. Preparations from fiber cells which form the cortex of the same lenses revealed the presence of two domains only, the phospholipid bilayer saturated with Chol and the CBD. The high Chol content in these aged nuclear membranes (with a Chol/PL molar ratio of 4.4) exceeded the evaluated CST value of 1.8 and thus is likely to have contributed to the formation of Chol crystals. The Chol/PL ratio for cortical membranes was 1.8, and the evaluated CST value was 1.76. The Chol content (expressed as the Chol/PL molar ratio) of cortical and nuclear membranes in lenses of 41–60-year-old donors was 1.38 and 2.1, respectively, and the evaluated CST value was 1.76 and 1.78, respectively. The small number of samples and the limited sensitivity of the DSC approach (discussed in the section “Detection of cholesterol crystals”) were the reasons Chol crystals were not detected in samples when the amount of Chol only slightly exceeded the CST.

We also compared the properties of lens-lipid membranes prepared from the total lipids extracted from cataractous lenses with those from age-matched clear lenses. Cataractous lenses were also obtained from 61–70-year-old donors. The Chol content of both cortical and nuclear membranes of cataractous lenses was substantially lower than that of cortical and nuclear membranes of clear lenses. These amounts were also lower than the evaluated CST values (discussed in the section “Detection of cholesterol crystals”). Thus, formation of Chol crystals in these membrane suspensions was not expected. Because of the low Chol content, the amount and the size of CBDs formed in cataractous lens-lipid membranes also decreased (discussed in the section “Discrimination of CBDs by use of saturation-recovery EPR with Chol analog spin labels”). This effect was clearly seen for cortical cataractous membranes, for which the Chol/PL molar ratio was 1.14—substantially lower than the evaluated CST value of 2.0. In nuclear cataractous membranes, this difference was also significant for the Chol/PL molar ratio of 1.45 and the evaluated CST value of 1.84. These values were equal in cortical membranes of clear lenses, and the Chol content substantially exceeded the CST value for nuclear membranes. All these differences are illustrated schematically in Fig. 7.

Our results indicate that high Chol content, formation of CBDs and formation of Chol crystals did not affect the clarity of lenses from 61–70-year-old donors. Membranes of cataractous lenses from the same age group contained a much smaller amount of Chol, smaller CBDs, and no Chol crystals. In a recent review we discussed the functions of Chol and the CBD specific to the fiber cell plasma membrane of the eye lens (Subczynski et al. 2012). The major conclusion was that the high Chol content and the presence of the CBD help to maintain lens membrane homeostasis when the membrane phospholipid composition changes substantially. The lipid-bilayer membrane saturated with Chol serves as an impermeable barrier to water and ions and as a matrix for major lens membrane proteins that are necessary for control of water and ion homeostasis. All of these are required for maintenance of lens clarity. Thus, high Chol and CBDs have beneficial functions for eye lenses. It is unlikely, however, that formation of Chol crystals can be regarded as beneficial. Our results indicated that formation of Chol crystals is not harmful for aged lenses. The unique structure of the lens protects it from the harmful induction of inflammasomes (maturated fiber cells do not contain intracellular organelles) and from initiation of the inflammatory cascade (the lens is avascular). Thus, Chol crystals can be formed without harmful effects on lens properties (clarity) and functions. All these factors suggest that the high Chol content, formation of CBDs, and formation of Chol crystals should not be regarded as major predispositions for the development of age-related cataracts.

Because of low cell turnover, cells in the nucleus of the human lens may be regarded the longest lived cells in our bodies (as old as the individual). Consequently, they require functional mechanisms to protect them from age-related damage. Indeed, the lipid composition of human lens membranes undergoes drastic changes with age, which are not observed for membranes of other organs and tissues. Phospholipid composition changes substantially with age, with an increase of sphingolipid content and depletion of phosphatidylcholine (Borchman et al. 1994; Deeley et al. 2008; Yappert and Borchman 2004; Yappert et al. 2003). The level of saturation of phospholipid alkyl-chains also increases (Deeley et al. 2008; Li et al. 1985; Yappert et al. 2003). Most characteristic is the increase in Chol content up to a Chol/PL ratio of 4 (Li et al. 1985, 1987; Rujoi et al. 2003; Zelenka 1984). Can the unique composition and the drastic changes in the lipid composition be regarded as protective mechanisms against age-related damage? This composition ensures chemical stability of the membrane components. It also ensures high structural stability of lipid membranes. Sphingolipids, which are extremely abundant in human eye lens membranes and only increase with age, can bind more tightly to neighboring phospholipids and Chol, increasing the stability and rigidity of membranes (Yappert and Borchman 2004). The saturating Chol content of fiber cell membranes, which also increases with age, keeps the bulk physical properties of lens-lipid membranes consistent and independent of age-related changes in phospholipid composition (Subczynski et al. 2012).

All these age-related compositional changes are beneficial for lens function. Can they be considered as protective mechanisms developed by nature? We assume that changes in lens properties beyond the age of 50 are not beneficial. As indicated by Borchman and co-authors (Borchman et al. 1994; Deeley et al. 2008; Yappert and Borchman 2004; Yappert et al. 2003), the increase in the sphingolipid content and the depletion of phosphatidylcholine leveled off after the age of 40–50. However, Chol content increases beyond that age,

forming CBDs and Chol crystals in aged fiber cells. We do not consider this age-related process is harmful. So, studying age-related changes should help us to better understand their positive and negative effect on lens function, and enable researchers to develop strategies which should enhance the positive effects and diminish the negative effects of aging.

Acknowledgments

This work was supported by grants EY015526, EB002052, EB001980, and EY001931 from the National Institutes of Health. We acknowledge the help of Bhavna Sheth, MD.

References

Bach D, Wachtel E. Phospholipid/cholesterol model membranes: formation of cholesterol crystallites. Biochim Biophys Acta. 2003; 1610:187–197. [PubMed: 12648773]

Benatti CR, Lamy MT, Epand RM. Cationic amphiphiles and the solubilization of cholesterol crystallites in membrane bilayers. Biochim Biophys Acta. 2008; 1778:844–853. [PubMed: 18201547]

Borchman D, Delamere NA, Cauley LA, Paterson CA. Studies on the distribution of cholesterol, phospholipid and protein in the human and bovine lens. Lens Eye Toxic Res. 1989; 6:703–724. [PubMed: 2487279]

Borchman D, Lamba OP, Yappert MC. Structural characterization of lipid membranes from clear and cataractous human lenses. Exp Eye Res. 1993; 57:199–208. [PubMed: 8405186]

Borchman D, Byrdwell WC, Yappert MC. Regional and age-dependent differences in the phospholipid composition of human lens membranes. Invest Ophthalmol Vis Sci. 1994; 35:3938–3942. [PubMed: 7928192]

Borchman D, Cenedella RJ, Lamba OP. Role of cholesterol in the structural order of lens membrane lipids. Exp Eye Res. 1996; 62:191–197. [PubMed: 8698079]

Buboltz JT. A more efficient device for preparing model-membrane liposomes by the rapid solvent exchange method. Rev Sci Instrum. 2009; 80:124301. [PubMed: 20059155]

Buboltz JT, Feigenson GW. A novel strategy for the preparation of liposomes: rapid solvent exchange. Biochim Biophys Acta. 1999; 1417:232–245. [PubMed: 10082799]

Cenedella RJ. Cholesterol and cataracts. Surv Ophthalmol. 1996; 40:320–337. [PubMed: 8658343]

de Vries AC, Cohen LH. Different effects of the hypolipidemic drugs pravastatin and lovastatin on the cholesterol biosynthesis of the human ocular lens in organ culture and on the cholesterol content of the rat lens in vivo. Biochim Biophys Acta. 1993; 1167:63–69. [PubMed: 8461334]

Deeley JM, Mitchell TW, Wei X, Korth J, Nealon JR, Blanksby SJ, Truscott RJ. Human lens lipids differ markedly from those of commonly used experimental animals. Biochim Biophys Acta. 2008; 1781:288–298. [PubMed: 18474264]

Devaux, PF. ESR and NMR studies of lipid-protein interactions in membranes.. In: Berliner, LJ.; Reuben, J., editors. Biological magnetic resonance. Plenum Press; New York: 1983. p. 183-299.

Epand RM. Cholesterol in bilayers of sphingomyelin or dihydrosphingomyelin at concentrations found in ocular lens membranes. Biophys J. 2003; 84:3102–3110. [PubMed: 12719240]

Estrada R, Yappert MC. Regional phospholipid analysis of porcine lens membranes by matrix-assisted laser desorption/ ionization time-of-flight mass spectrometry. J Mass Spectrom. 2004; 39:1531–1540. [PubMed: 15578747]

Folch J, Lees M, Sloane Stanley GH. A simple method for the isolation and purification of total lipids from animal tissues. J Biol Chem. 1957; 226:497–509. [PubMed: 13428781]

Huang J, Buboltz JT, Feigenson GW. Maximum solubility of cholesterol in phosphatidylcholine and phosphatidylethanolamine bilayers. Biochim Biophys Acta. 1999; 1417:89–100. [PubMed: 10076038]

Huang L, Grami V, Marrero Y, Tang D, Yappert MC, Rasi V, Borchman D. Human lens phospholipid changes with age and cataract. Invest Ophthalmol Vis Sci. 2005; 46:1682–1689. [PubMed: 15851569]

Jacob RF, Cenedella RJ, Mason RP. Direct evidence for immiscible cholesterol domains in human ocular lens fiber cell plasma membranes. J Biol Chem. 1999; 274:31613–31618. [PubMed: 10531368]

Jacob RF, Cenedella RJ, Mason RP. Evidence for distinct cholesterol domains in fiber cell membranes from cataractous human lenses. J Biol Chem. 2001; 276:13573–13578. [PubMed: 11278611]

Kawasaki K, Yin J-J, Subczynski WK, Hyde JS, Kusumi A. Pulse EPR detection of lipid exchange between protein rich raft and bulk domains in the membrane: methodology development and its application to studies of influenza viral membrane. Biophys J. 2001; 80:738–748. [PubMed: 11159441]

Kirby TJ. Cataracts produced by triparanol. (MER-29). Trans Am Ophthalmol Soc. 1967; 65:494–543. [PubMed: 4230196]

Kusumi A, Subczynski WK, Hyde JS. Oxygen transport parameter in membranes as deduced by saturation recovery measurements of spin-lattice relaxation times of spin labels. Proc Natl Acad Sci USA. 1982; 79:1854–1858. [PubMed: 6952236]

Lai CL, Shau WY, Chang CH, Chen MF, Lai MS. Statin use and cataract surgery: a nationwide retrospective cohort study in elderly ethnic Chinese patients. Drug Saf. 2013; 36:1017–1024. [PubMed: 23771795]

Leuschen J, Mortensen EM, Frei CR, Mansi EA, Panday V, Mansi I. Association of statin use with cataracts: a propensity score-matched analysis. JAMA Ophthalmol. 2013; 131:1427–1434. [PubMed: 24052188]

Li LK, So L, Spector A. Membrane cholesterol and phospholipid in consecutive concentric sections of human lenses. J Lipid Res. 1985; 26:600–609. [PubMed: 4020298]

Li LK, So L, Spector A. Age-dependent changes in the distribution and concentration of human lens cholesterol and phospholipids. Biochim Biophys Acta. 1987; 917:112–120. [PubMed: 3790601]

Loomis CR, Shipley GG, Small DM. The phase behavior of hydrated cholesterol. J Lipid Res. 1979; 20:525–535. [PubMed: 458269]

Machan CM, Hrynchak PK, Irving EL. Age-related cataract is associated with type 2 diabetes and statin use. Optom Vis Sci. 2012; 89:1165–1171. [PubMed: 22797512]

Mailer C, Nielsen RD, Robinson BH. Explanation of spin-lattice relaxation rates of spin labels obtained with multifrequency saturation recovery EPR. J Phys Chem A. 2005; 109:4049–4061. [PubMed: 16833727]

Mainali L, Feix JB, Hyde JS, Subczynski WK. Membrane fluidity profiles as deduced by saturation-recovery EPR measurements of spin-lattice relaxation times of spin labels. J Magn Reson. 2011a; 212:418–425. [PubMed: 21868272]

Mainali L, Raguz M, Camenisch TG, Hyde JS, Subczynski WK. Spin-label saturation-recovery EPR at W-band: applications to eye lens-lipid membranes. J Magn Reson. 2011b; 212:86–94. [PubMed: 21745756]

Mainali L, Raguz M, O'Brien WJ, Subczynski WK. Properties of fiber cell plasma membranes isolated from the cortex and nucleus of the porcine eye lens. Exp Eye Res. 2012a; 97:117–129. [PubMed: 22326289]

Mainali L, Raguz M, Subczynski WK. Phases and domains in sphingomyelin-cholesterol membranes: structure and properties using EPR spin-labeling methods. Eur Biophys J. 2012b; 41:147–159. [PubMed: 22033879]

Mainali L, Hyde JS, Subczynski WK. Using spin-label W-band EPR to study membrane fluidity profiles in samples of small volume. J Magn Reson. 2013a; 226:35–44. [PubMed: 23207176]

Mainali L, Raguz M, O'Brien WJ, Subczynski WK. Properties of membranes derived from the total lipids extracted from the human lens cortex and nucleus. Biochim Biophys Acta. 2013b; 1828:1432–1440. [PubMed: 23438364]

Mainali L, Raguz M, Subczynski WK. Formation of cholesterol bilayer domains precedes formation of cholesterol crystals in cholesterol/dimyristoylphosphatidylcholine membranes: EPR and DSC studies. J Phys Chem B. 2013c; 117:8994–9003. [PubMed: 23834375]

Mainali L, Sidabras JW, Camenisch TG, Ratke JJ, Raguz M, Hyde JS, Subczynski WK. Spin-label W-band EPR with seven-loop–six-gap resonator: application to lens membranes derived from eyes of a single donor. Appl Magn Reson. 2014; 45:1343–1358. [PubMed: 25541571]

Marsh, D. Electron spin resonance: spin labels.. In: Grell, E., editor. Membrane spectroscopy. Springer; Berlin: 1981. p. 51-142.

Mason RP, Jacob RF. Membrane microdomains and vascular biology. Emerging role in atherogenesis. Circulation. 2003; 107:2270–2273. [PubMed: 12732593]

Mason R, Tulenko TN, Jacob RF. Direct evidence for cholesterol crystalline domains in biological membranes: role in human pathobiology. Biochim Biophys Acta. 2003; 1610:198–207. [PubMed: 12648774]

Mosley ST, Kalinowski SS, Schafer BL, Tanaka RD. Tissue-selective acute effects of inhibitors of 3-hydroxy-3-methylglutaryl coenzyme A reductase on cholesterol biosynthesis in lens. J Lipid Res. 1989; 30:1411–1420. [PubMed: 2513368]

Paterson CA, Zeng J, Husseini Z, Borchman D, Delamere NA, Garland D, Jimenez-Asensio J. Calcium ATPase activity and membrane structure in clear and cataractous human lenses. Curr Eye Res. 1997; 16:333–338. [PubMed: 9134322]

Plesnar E, Subczynski WK, Pasenkiewicz-Gierula M. Saturation with cholesterol increases vertical order and smoothes the surface of the phosphatidylcholine bilayer: a molecular simulation study. Biochim Biophys Acta. 2012; 1818:520–529. [PubMed: 22062420]

Raguz M, Widomska J, Dillon J, Gaillard ER, Subczynski WK. Characterization of lipid domains in reconstituted porcine lens membranes using EPR spin-labeling approaches. Biochim Biophys Acta. 2008; 1778:1079–1090. [PubMed: 18298944]

Raguz M, Widomska J, Dillon J, Gaillard ER, Subczynski WK. Physical properties of the lipid bilayer membrane made of cortical and nuclear bovine lens-lipids: EPR spin-labeling studies. Biochim Biophys Acta. 2009; 1788:2380–2388. [PubMed: 19761756]

Raguz M, Mainali L, Widomska J, Subczynski WK. The immiscible cholesterol bilayer domain exists as an integral part of phospholipid bilayer membranes. Biochim Biophys Acta. 2011a; 1808:1072–1080. [PubMed: 21192917]

Raguz M, Mainali L, Widomska J, Subczynski WK. Using spin-label electron paramagnetic resonance (EPR) to discriminate and characterize the cholesterol bilayer domain. Chem Phys Lipids. 2011b; 164:819–829. [PubMed: 21855534]

Raguz M, Mainali L, O'Brien WJ, Subczynski WK. Lipid-protein interactions in plasma membranes of fiber cells isolated from the human eye lens. Exp Eye Res. 2014; 120:138–151. [PubMed: 24486794]

Robinson BH, Haas DA, Mailer C. Molecular dynamics in liquids: spin-lattice relaxation of nitroxide spin labels. Science. 1994; 263:490–493. [PubMed: 8290958]

Rujoi M, Jin J, Borchman D, Tang D, Yappert MC. Isolation and lipid characterization of cholesterol-enriched fractions in cortical and nuclear human lens fibers. Invest Ophthalmol Vis Sci. 2003; 44:1634–1642. [PubMed: 12657603]

Schreier S, Polnaszek CF, Smith IC. Spin labels in membranes. Problems in practice. Biochim Biophys Acta. 1978; 515:395–436. [PubMed: 215206]

Shaikh SR, Cherezov V, Caffrey M, Soni SP, LoCascio D, Stillwell W, Wassall SR. Molecular organization of cholesterol in unsaturated phosphatidylethanolamines: X-ray diffraction and solid state 2H NMR reveal differences with phosphatidylcho-lines. J Am Chem Soc. 2006; 128:5375–5383. [PubMed: 16620109]

Subczynski WK, Hyde JS, Kusumi A. Oxygen permeability of phosphatidylcholine-cholesterol membranes. Proc Natl Acad Sci USA. 1989; 86:4474–4478. [PubMed: 2543978]

Subczynski WK, Hyde JS, Kusumi A. Effect of alkyl chain unsaturation and cholesterol intercalation on oxygen transport in membranes: a pulse ESR spin labeling study. Biochemistry. 1991; 30:8578–8590. [PubMed: 1653601]

Subczynski WK, Hopwood LE, Hyde JS. Is the mammalian cell plasma membrane a barrier to oxygen transport? J Gen Physiol. 1992; 100:69–87. [PubMed: 1324973]

Subczynski WK, Wisniewska A, Yin J-J, Hyde JS, Kusumi A. Hydrophobic barriers of lipid bilayer membranes formed by reduction of water penetration by alkyl-chain unsaturation and cholesterol. Biochemistry. 1994; 33:7670–7681. [PubMed: 8011634]

Subczynski WK, Felix CC, Klug CS, Hyde JS. Concentration by centrifugation for gas exchange EPR oximetry measurements with loop-gap resonators. J Magn Reson. 2005; 176:244–248. [PubMed: 16040261]

Subczynski WK, Raguz M, Widomska J. Studying lipid organization in biological membranes using liposomes and EPR spin labeling. Methods Mol Biol. 2010; 606:247–269. [PubMed: 20013402]

Subczynski WK, Raguz M, Widomska J, Mainali L, Konovalov A. Functions of cholesterol and the cholesterol bilayer domain specific to the fiber-cell plasma membrane of the eye lens. J Membr Biol. 2012; 245:51–68. [PubMed: 22207480]

Tulenko TN, Chen M, Mason PE, Mason RP. Physical effects of cholesterol on arterial smooth muscle membranes: evidence of immiscible cholesterol domains and alterations in bilayer width during atherogenesis. J Lipid Res. 1998; 39:947–956. [PubMed: 9610760]

Widomska J, Raguz M, Dillon J, Gaillard ER, Subczynski WK. Physical properties of the lipid bilayer membrane made of calf lens lipids: EPR spin labeling studies. Biochim Biophys Acta. 2007; 1768:1454–1465. [PubMed: 17451639]

Yappert MC, Borchman D. Sphingolipids in human lens membranes: an update on their composition and possible biological implications. Chem Phys Lipids. 2004; 129:1–20. [PubMed: 14998723]

Yappert MC, Rujoi M, Borchman D, Vorobyov I, Estrada R. Glycero-versus sphingo-phospholipids: correlations with human and non-human mammalian lens growth. Exp Eye Res. 2003; 76:725–734. [PubMed: 12742355]

Yin JJ, Subczynski WK. Effects of lutein and cholesterol on alkyl chain bending in lipid bilayers: a pulse electron spin resonance spin labeling study. Biophys J. 1996; 71:832–839. [PubMed: 8842221]

Zelenka PS. Lens lipids. Curr Eye Res. 1984; 3:1337–1359. [PubMed: 6391828]

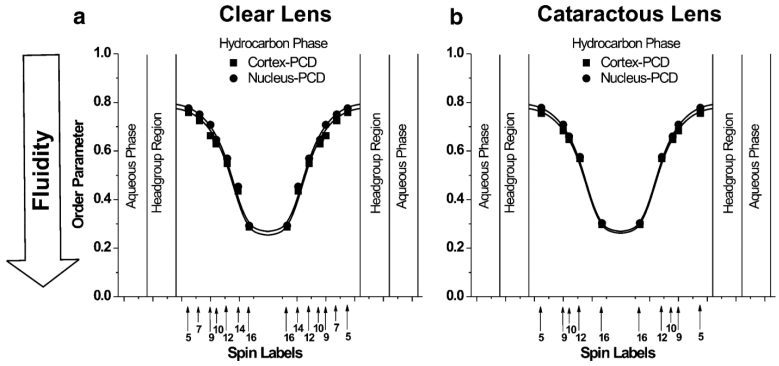

Fig. 1.

Profiles of the order parameter across the phospholipid–cholesterol domain (PCD) of cortical and nuclear lens-lipid membranes of clear (**a**) and cataractous (**b**) human lenses obtained at 37 °C with phospholipid-type spin labels. Approximate locations of the nitroxide groups of spin labels are indicated by *arrows*

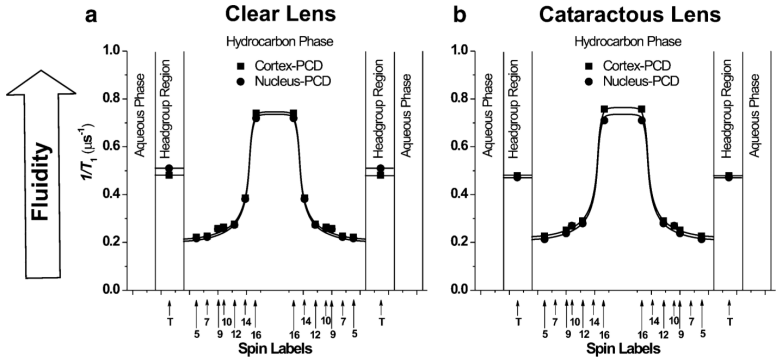

Fig. 2.

Profiles of T^{-1}_1 (the spin–lattice relaxation rate) across the phospholipid–cholesterol domain (PCD) of cortical and nuclear lens-lipid membranes of clear (**a**) and cataractous (**b**) human lenses obtained at 37 °C with phospholipid-type spin labels. Approximate locations of the nitroxide groups of spin labels are indicated by *arrows*

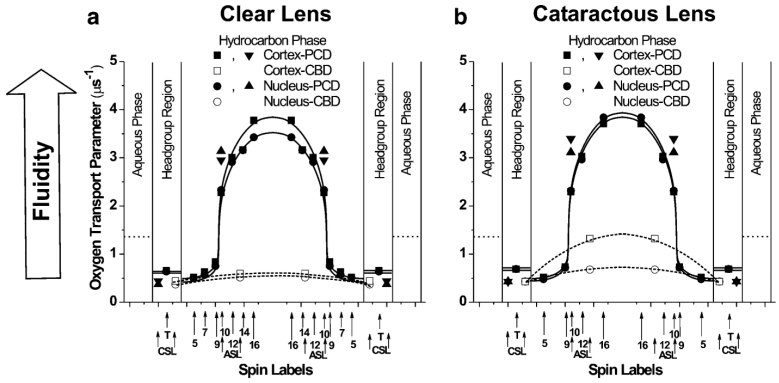

Fig. 3.

Profiles of the oxygen transport parameter across the phospholipid–cholesterol domain (PCD) of cortical and nuclear lens-lipid membranes of clear (**a**) and cataractous (**b**) human lenses obtained at 37 °C with phospholipid-type and cholesterol-type spin labels, and across the CBD with cholesterol-type spin labels. Approximate locations of the nitroxide groups of spin labels are indicated by *arrows*

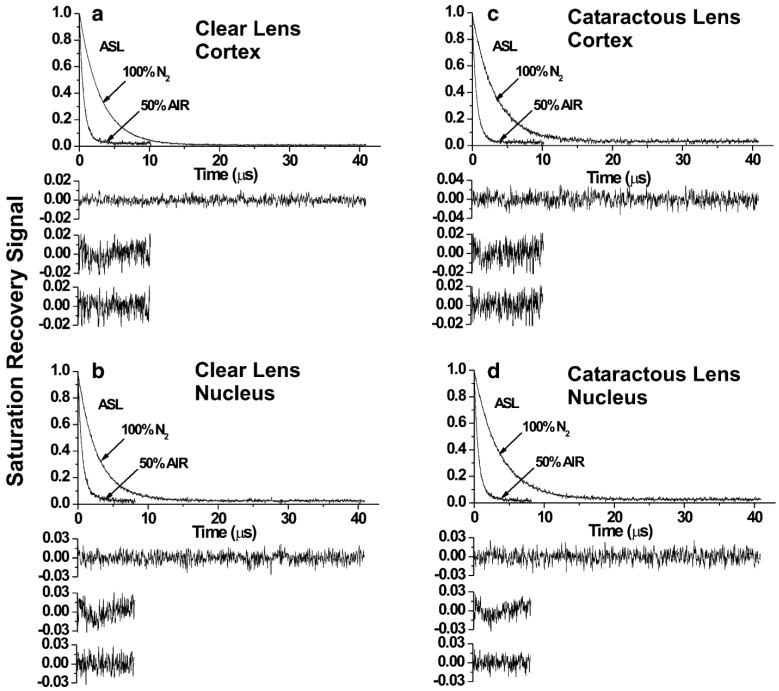

Fig. 4.

Saturation-recovery signals with fitted curves and residuals for ASL for clear (**a**, **b**) and cataractous (**c**, **d**) cortical (**a**, **c**) and nuclear (**b**, **d**) lens-lipid membranes. Signals were recorded for samples equilibrated with 100 % nitrogen and a gas mixture of 50 % air and 50 % nitrogen (as indicated in the figures). For deoxygenated samples, saturation-recovery signals were satisfactorily fit to a single-exponential function with time constants of **a** 3.02 ± 0.01 μs, **b** 2.79 ± 0.01 μs, **c** 3.27 ± 0.01 μs, and **d** 3.57 ± 0.01 μs (upper residuals are for single-exponential fit). The saturation-recovery signal for ASL in the presence of molecular oxygen can be fitted satisfactorily only with double-exponential curves with time constants of **a** 1.33 ± 0.18 and 0.55 ± 0.01 μs, **b** 1.61 ± 0.14 and 0.52 ± 0.01 μs, **c** 0.89 ± 0.10 and 0.49 ± 0.04 μs, and **d** 1.86 ± 0.18 and 0.53 ± 0.01 μs (the middle and lower residuals are for single-exponential and double-exponential fits)

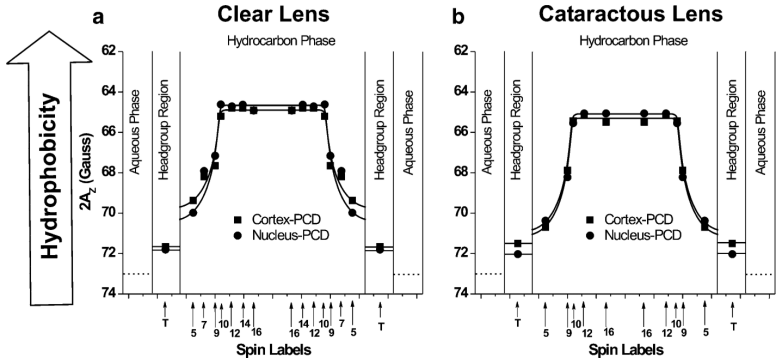

Fig. 5.

Profiles of hydrophobicity ($2A_Z$) across the phospholipid–cholesterol domain (PCD) of cortical and nuclear lens-lipid membranes of clear (**a**) and cataractous (**b**) human lenses obtained at 37 °C with phospholipid-type spin labels. Approximate locations of the nitroxide groups of spin labels are indicated by *arrows*

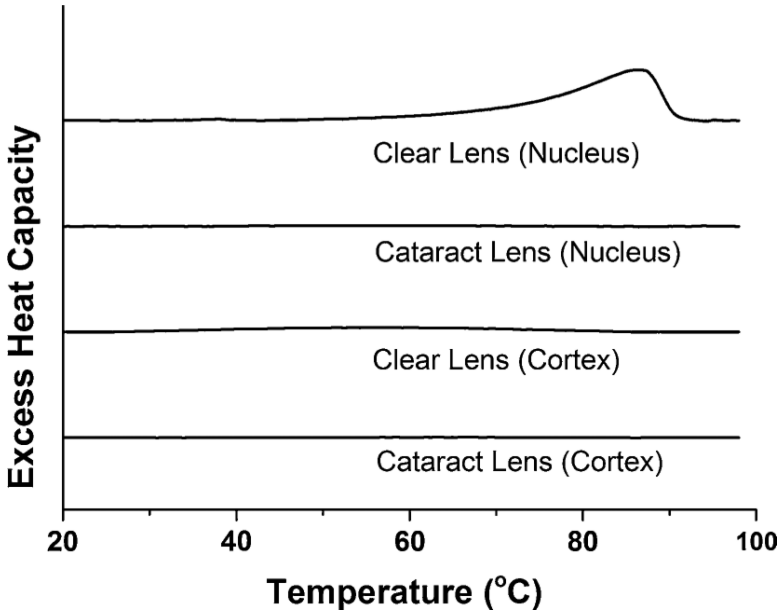

Fig. 6.

First DSC heating scans of cortical and nuclear membrane dispersions of clear and cataractous lenses

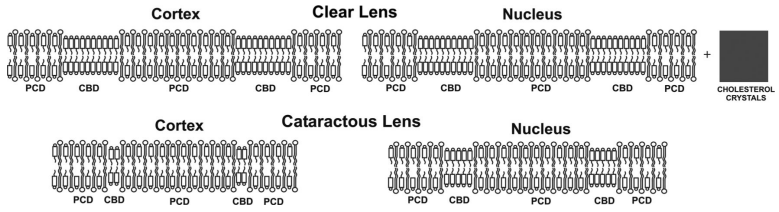

Fig. 7.

Schematic drawing of clear (**a**) and cataractous (**b**) cortical and nuclear lens-lipid membranes containing the bulk phospholipid–cholesterol bilayer (PCD) and the pure cholesterol bilayer domain (CBD), with the cholesterol crystals (for the clear nuclear lens-lipid membrane)

Table 1

Oxygen transport parameter and NiEDDA accessibility parameter measured with ASL and CSL in domains of the clear and cataractous human lens-lipid membrane at 37 °C

	Oxygen transport parameter		NiEDDA accessibility parameter	
	ASL (μs^{-1})	CSL (μs^{-1})	ASL (μs^{-1})	CSL (μs^{-1})
Clear lens				
Phospholipid–cholesterol domain in cortical membrane	2.95	0.44	0.003	0.37
Cholesterol bilayer domain in cortical membrane	0.60	0.44	0.003	1.92
Phospholipid–cholesterol domain in nuclear membrane	3.14	0.37	0.004	0.34
Cholesterol bilayer domain in nuclear membrane	0.52	0.37	0.004	1.83
Cataractous lens				
Phospholipid–cholesterol domain in cortical membrane	3.40	0.43	0.005	0.33
Cholesterol bilayer domain in cortical membrane	1.32	0.43	0.005	1.48
Phospholipid–cholesterol domain in nuclear membrane	3.11	0.43	0.003	0.35
Cholesterol bilayer domain in nuclear membrane	0.68	0.43	0.003	1.77